# Phenomenological consequences of singlet neutrinos

Lay Nam Chang*

*Institute for High Energy Physics, Virginia Polytechnic Institute and State University, Blacksburg, Virginia 24061-0435*

Daniel Ng and John N. Ng

*TRIUMF, 4004 Wesbrook Mall, Vancouver, British Columbia, V6T 2A3, Canada*

In this paper, we study the phenomenology of right-handed neutrino isosinglets. We consider the general situation where the neutrino masses are not necessarily given by $m_D^2/M$, where $m_D$ and $M$ are the Dirac and Majorana mass terms, respectively. The consequent mixing between the light and heavy neutrinos is then not suppressed, and we treat it as an independent parameter in the analysis. It turns out that $\mu$-$e$ conversion is an important experiment in placing limits on the heavy mass scale ($M$) and the mixing. Mixings among light neutrinos are constrained by neutrinoless double-$\beta$ decay, as well as by solar and atmospheric neutrino experiments. Detailed one-loop calculations for lepton-number-violating vertices are provided.

PACS number(s): 14.60.St, 13.35.Bv, 14.60.Pq, 23.40.Bw

## I. INTRODUCTION

There is no direct evidence so far that neutrinos have mass. Indirectly, however, measurements on solar neutrino fluxes suggest that indeed they do have mass, albeit at values which are considerably smaller than those for charged fermions [1]. Within the standard model, this situation is accommodated quite naturally by restricting Higgs fields to the usual isodoublets, so that there are no direct Yukawa couplings among the left-handed lepton fields and scalar bosons. Nevertheless, gravity effects could induce a dimension five operator, but these would imply Majorana neutrino masses of the order $m_\nu \sim v^2/M_{Pl} \sim 10^{-5}$ eV, where $v = 250$ GeV is the scale of electroweak breaking and $M_{Pl} = 10^{19}$ GeV is the Planck mass. In what follows, we will ignore such contributions.

Generating neutrino masses poses somewhat different problems from those for charged fermions. This is primarily because neutral fermions could acquire Majorana masses, and so the whole question of mixing angles and their attendant $CP$ phases needs to be reexamined [2]. The most elementary way of generating neutrino masses would be through the introduction of neutral electroweak singlet fermion fields into the theory. Detecting finite masses for neutrinos therefore would provide a direct way for probing structure and dynamics beyond those of the standard model.

Right-handed neutrinos, which are electroweak singlet fermions, can have gauge-invariant Majorana masses $M$. The presence of a Higgs isodoublet induces Yukawa couplings of left- and right-handed neutrinos. Thus, left-

and right-handed neutrinos are linked together by Dirac masses $m_D$. The left-handed neutrinos acquire their Majorana masses, given by $m_\nu = m_D^2/M$, when we integrate out the heavy right-handed neutrinos. This is called the "seesaw" mechanism [3]. The mixing of the left- to the right-handed neutrinos, given by $m_D/M$, can be rewritten as $\sqrt{m_\nu/M}$. As a result, exotic processes, such as $\mu \to e\gamma$, $\mu \to 3e$, and $\mu$-$e$ conversion in nuclei, are very suppressed by the smallness of light neutrino masses.

In the analysis to be presented below, we consider the situation where the light neutrinos are not given by $m_D^2/M$. This is possible when there is more than one right-handed neutrino. Hence, the mixing $m_D/M$ will be independent of the light neutrino masses. Within such a context, it will be sufficient for three generations of left-handed neutrinos and an additional right-handed neutrino field $\nu^c$ to illustrate the kinds of bounds on neutrino masses and mixings that can be extracted from existing data. This model, suggested by Jarlskog in Ref. [4], can be considered a remnant of some higher energy theory manifested at the current low energy scale, and $\nu^c$ as an effective collection of an arbitrary number of right-handed neutrino fields.

The presence of $\nu^c$ can give rise to much interesting phenomenology. In addition to neutrino masses and mixings, there can be lepton-family-number-violating processes, violations of generation universality, and off-diagonal neutral current couplings. In this paper, we will consider this phenomenology in detail, and examine how available data constrain the parameters in this scenario. $CP$ violation will not be considered here. We first formulate the model in Sec. II. Constraints of the model, obtained from $Z$ decays and universalities in charged current processes, are given in Sec. III. In Secs. IV and V, we use the information obtained in Sec. III to calculate lepton-family-number-violating processes and neutrinoless double-$\beta$ decay. In Sec. VI, we discuss neutrino oscil-

lations. Finally, we will conclude our analysis in Sec. VII. Although the model we are studying is not new, to the best of our knowledge, the idea of relaxing the seesaw mass relationship has not been studied in detail. In addition, the results on rare decays have not been presented before.

$$\mathcal{L}_Y(\nu^c) = -\frac{g}{\sqrt{2}m_W} \sum_{\alpha=e,\mu,\tau} a_\alpha \left( \overline{\nu_\alpha} \quad \overline{\alpha_L} \right) \left( \begin{array}{c} \frac{1}{\sqrt{2}}(H^0 - iG^0) \\ -G^- \end{array} \right) \overline{\nu^c} + \text{H.c.} ,$$  (2.1)

where $a$'s are assumed to be real. Without losing any generality, we can define the charged leptons $\alpha_L$ to be given by their mass eigenstates. Since $\nu^c$ is a gauge singlet of the standard model, it can pick up a Majorana mass:

$$\mathcal{L}_{\text{mass}}(\nu^c) = -\frac{1}{2}M\nu^c \nu^c + \text{H.c.}$$  (2.2)

$\nu_\alpha$ and $\nu^c$ are the two-component Weyl fields. When the SU(2) × U(1) gauge symmetry of the standard model is broken spontaneously, mixings among the gauge eigenstates $\nu_\alpha$ and $\nu^c$ are induced, leading to the mass matrix [4]

$$\frac{1}{2} \left( \nu_e \quad \nu_\mu \quad \nu_\tau \quad \nu^c \right) \mathcal{M} \left( \begin{array}{c} \nu_e \\ \nu_\mu \\ \nu_\tau \\ \nu^c \end{array} \right) + \text{H.c.} ,$$  (2.3)

where

$$\mathcal{M} = \left( \begin{array}{cccc} 0 & 0 & 0 & a_e \\ 0 & 0 & 0 & a_\mu \\ 0 & 0 & 0 & a_\tau \\ a_e & a_\mu & a_\tau & M \end{array} \right) .$$  (2.4)

$\mathcal{M}$ can be diagonalized by a rotational matrix $\mathcal{O}$:

$$\mathcal{O}^T \mathcal{M} \mathcal{O} = \left( \begin{array}{cccc} 0 & 0 & 0 & 0 \\ 0 & 0 & 0 & 0 \\ 0 & 0 & m_3 & 0 \\ 0 & 0 & 0 & m_4 \end{array} \right) .$$  (2.5)

$\mathcal{O}$, defined as $\nu_\alpha = \sum_{i=1}^{4} \mathcal{O}_{\alpha i}\nu_i$ ($\alpha = e, \mu, \tau$, and $R$), is explicitly given by

$$\mathcal{O} = \left( \begin{array}{cccc} c_1 & s_1c_2 & s_1s_2c_3 & s_1s_2s_3 \\ -s_1 & c_1c_2 & c_1s_2c_3 & c_1s_2s_3 \\ 0 & -s_2 & c_2c_3 & c_2s_3 \\ 0 & 0 & -s_3 & c_3 \end{array} \right) \left( \begin{array}{cccc} 1 & 0 & 0 & 0 \\ 0 & 1 & 0 & 0 \\ 0 & 0 & i & 0 \\ 0 & 0 & 0 & 1 \end{array} \right) ,$$  (2.6)

where we adopt the abbreviation $s_i = \sin\theta_i$ and $c_i = \cos\theta_i$.

## II. FORMULATION OF THE ONE SINGLET MODEL

When one $\nu^c$ is added to the standard model, the new Yukawa interactions that must be included are given by

Equation (2.6) is defined in a way that both eigen-masses $m_3$ and $m_4$ are positive. The $i$ in Eq. (2.6) indicates that $\nu_3$ and $\nu_4$ have opposite $CP$ transformation. The mixing angles among the light neutrinos are given by

$$s_1 = \frac{a_e}{\sqrt{a_e^2 + a_\mu^2}}, \quad s_2 = \frac{\sqrt{a_e^2 + a_\mu^2}}{\sqrt{a_e^2 + a_\mu^2 + a_\tau^2}} ,$$  (2.7)

whereas the mixing between the light and heavy neutrinos is

$$s_3^2 = \frac{m_3}{m_3 + m_4} .$$  (2.8)

The masses for the two massive neutrinos are given as

$$m_3 = \frac{-M + \sqrt{M^2 + 4(a_e^2 + a_\mu^2 + a_\tau^2)}}{2} ,$$  (2.9)

$$m_4 = \frac{M + \sqrt{M^2 + 4(a_e^2 + a_\mu^2 + a_\tau^2)}}{2} .$$  (2.10)

The diagonalization condition, Eq. (2.5), is used when we calculate the $Z$ penguin diagrams; see Appendix B. Note that for $M^2 \gg (a_e^2 + a_\mu^2 + a_\tau^2)$, we have the seesaw mass for $\nu_3$, $m_3 \sim (a_e^2 + a_\mu^2 + a_\tau^2)/M$.

Notice that $s_3$ is suppressed by the square root of the ratio of light to heavy neutrino masses, in accordance with the general arguments presented in the Introduction. As we have already pointed out there, to avoid such a suppression, one requires more than one right-handed neutrino state. When there is more than one right-handed neutrino, seesaw relationships, Eq. (2.8) and (2.9), do not necessarily hold. We furnish details on how this can come about in Appendix A. In what follows, we shall accommodate such an eventuality by treating $s_3$ as an independent parameter and continue to consider $\nu^c$ as an effective collection of arbitrary number of right-handed neutrinos. This scenario may well be remnants of symmetries which are manifest at higher energies.

The consequent charged current interactions of the $W$ gauge boson, in four-component notation, are given by

$$\mathcal{L}_W = \frac{g}{\sqrt{2}} W_\mu^- \sum_{\alpha=e,\mu,\tau} \sum_{i=1,\ldots,4} \mathcal{O}_{\alpha i} \, \bar{\alpha} \, \gamma^\mu \frac{1-\gamma_5}{2} \, \nu_i + \text{H.c.}$$

(2.11)

The neutral current interactions of the $Z$ gauge boson can be obtained straightforwardly. The interaction remains the same as in the standard model for the charged leptons and remains flavor diagonal. However, there will be nondiagonal pieces induced by $\nu^c$. The interactions in four-component notation are given by

$$\mathcal{L}_{Z\bar{e}e} = \frac{g}{\cos\theta_W} Z_\mu \sum_{\alpha=e,\mu,\tau} \bar{\alpha} \, \gamma^\mu \left[ g_L \frac{1-\gamma_5}{2} + g_R \frac{1+\gamma_5}{2} \right] \alpha,$$

(2.12)

$$\mathcal{L}_{Z\bar{\nu}\nu} = \frac{g}{4\cos\theta_W} Z_\mu \sum_{i,j=1}^{4} \bar{\nu}_i \, \gamma^\mu \left[ L_{ij} \frac{1-\gamma_5}{2} + R_{ij} \frac{1+\gamma_5}{2} \right] \nu_j \, ,$$

(2.13)

where

$$g_L = -\frac{1}{2} + \sin^2\theta_W \, ,$$

(2.14a)

$$g_R = \sin^2\theta_W \, ,$$

(2.14b)

and

$$L_{ij} = \delta_{ij} - \mathcal{O}_{Ri}^* \mathcal{O}_{Rj} \, ,$$

(2.15a)

$$R_{ij} = -\delta_{ij} + \mathcal{O}_{Rj}^* \mathcal{O}_{Ri} \, .$$

(2.15b)

The interactions involving Goldstone bosons ($G^\pm$, $G^0$) and the physical Higgs scalar ($H^0$) can be obtained from Eq. (2.1), and, with the help of Eqs. (2.5), are given by

$$\mathcal{L}_{G^-} = \frac{g}{\sqrt{2}m_W} G^- \sum_{\alpha=e,\mu,\tau} \sum_{i=1,\ldots,4} \mathcal{O}_{\alpha i} \, m_i \, \bar{\alpha} \, \frac{1+\gamma_5}{2} \, \nu_i \, ,$$

(2.16)

$$\mathcal{L}_{G^0} = \frac{ig}{4m_W} G^0 \left[ \sum_{i=1,\ldots,4} m_i \, \nu_i^T C \gamma_5 \nu_i + \sum_{i,j=1,\ldots,4} M \left( \mathcal{O}_{Ri} \mathcal{O}_{Rj} \, \nu_i^T C \frac{1-\gamma_5}{2} \nu_j - \text{H.c.} \right) \right] \, ,$$

(2.17)

$$\mathcal{L}_{H^0} = -\frac{g}{4m_W} H^0 \left[ \sum_{i=1,\ldots,4} m_i \, \nu_i^T C \nu_i - \sum_{i,j=1,\ldots,4} M \left( \mathcal{O}_{Ri} \mathcal{O}_{Rj} \, \nu_i^T C \frac{1-\gamma_5}{2} \nu_j + \text{H.c.} \right) \right] \, .$$

(2.18)

From Eqs. (2.13), (2.17), and (2.18), we show explicitly the nondiagonal coupling induced by $\nu^c$. Using Eq. (2.6), these equations can be rewritten as

$$\mathcal{L}_{Z\bar{\nu}\nu} = -\frac{g}{4\cos\theta_W} Z_\mu \left[ \sum_{i=1,2} \bar{\nu}_i \gamma^\mu \gamma_5 \nu_i + c_3^2 \bar{\nu}_3 \gamma^\mu \gamma_5 \nu_3 + s_3^2 \bar{\nu}_4 \gamma^\mu \gamma_5 \nu_4 + 2is_3 c_3 \bar{\nu}_3 \gamma^\mu \nu_4 \right] \, ,$$

(2.19)

$$\mathcal{L}_{G^0} = \frac{ig}{4m_W} G^0 \left[ \sum_{i=1,\ldots,4} m_i \, \nu_i^T C \gamma_5 \nu_i + M \left( s_3^2 \nu_3^T C \gamma_5 \nu_3 - c_3^2 \nu_4^T C \gamma_5 \nu_4 - 2ic_3 s_3 \nu_3^T C \nu_4 \right) \right] \, ,$$

(2.20)

and

$$\mathcal{L}_{H^0} = -\frac{g}{4m_W} H^0 \left[ \sum_{i=1,\ldots,4} m_i \, \nu_i^T C \nu_i - M \left( -s_3^2 \nu_3^T C \nu_3 + c_3^2 \nu_4^T C \nu_4 + 2ic_3 s_3 \nu_3^T C \gamma_5 \nu_4 \right) \right] \, ,$$

(2.21)

respectively. Since $\nu_3$ and $\nu_4$ have opposite $CP$ because of the structure of the mass matrix we have assumed, the nondiagonal interactions in Eqs. (2.19)–(2.21) have different Lorentz structure from that of the diagonal terms. Hence, the charged-lepton-flavor-changing decays of $Z$ and $H^0$ may offer new channels to search for the existence of a right-handed neutrino.

## III. CONSTRAINTS OF THE MODEL

One of the predictions of this model is that two of the neutrinos ($\nu_{1,2}$) are massless at the tree level. These two massless neutrinos, which are not protected by symmetries, will pick up Majorana masses at higher order loops [5], but their eventual masses are negligibly small. For our purpose, we simply assume these two neutrinos to be massless. The other two neutrinos ($\nu_{3,4}$) are massive; we define $m_3 \leq m_4$. The decays of $\nu_4$ present us with a rich class of phenomena. To avoid any conflict with the cosmological and astrophysical constraints [6], we take $m_4$ to be greater than $\sim 1$ GeV.

As seen in Eq. (2.19), the presence of a right-handed singlet induces nondiagonal neutral currents among neutrinos. In addition, the strength of the $Z$-$\nu_3$-$\nu_3$ coupling is reduced by a factor of $c_3^2$ relative to $Z$-$\nu_1$-$\nu_1$ and the $Z$-$\nu_2$-$\nu_2$. Therefore, the invisible width of the $Z$ gauge boson will provide a stringent limit on the mixing parameters $s_3$. If $\nu_4$ is heavier than $Z$, $s_3$ can be constrained from the invisible width of the $Z$ gauge boson. A standard calculation using Eq. (2.19) modifies the formula for the effective number of light neutrino species [4,7] as measured by the CERN $e^+e^-$ collider LEP:

$$N_\nu = 2 + (1 - s_3^2)^2 . \tag{3.1}$$

At 90% C.L., $N_\nu$ is greater than 2.95 [8], leading to

$$s_3{}^2 \leq 2.69 \times 10^{-2} . \tag{3.2}$$

If $\nu_4$ is lighter than $Z$, the decays $Z \to \nu_3 \nu_4$ or $\nu_4 \nu_4$ are allowed. If $m_4$ is heavier than $\sim 1$ GeV, $\nu_4$ will decay within detectors, leaving exotic signatures such as $Z \to e \, \mu + X$. Recent experimental results on the search for lepton flavor violation in $Z$ decays can be found in Ref. [9]. The absence of these exotic signatures then provides a very stringent constraint on $s_3$. Since the decays of $\nu_4$ are so numerous, we use a conservative bound of

$$B(Z \to \nu_3\nu_4, \ \nu_4\nu_4) \leq 1 \times 10^{-5} \tag{3.3}$$

to constrain $s_3$. Combining Eqs. (3.1) and (3.3), we plot the upper bound on $s_3$ as a function of $m_4$ in Fig. 1.

Since $\nu_4$ is not kinematically allowed for the muon decay $\mu \to e\nu\nu$, only the first three neutrinos play a role. The Fermi coupling constant $G_F$ extracted from the muon lifetime is given by

$$\left(\frac{G_F}{\sqrt{2}}\right)^2 = \left(\frac{g^2}{8m_W^2}\right)^2 \left[1 - |\mathcal{O}_{e4}|^2\right]\left[1 - |\mathcal{O}_{\mu4}|^2\right] . \tag{3.4}$$

When radiative corrections are included in the on-shell
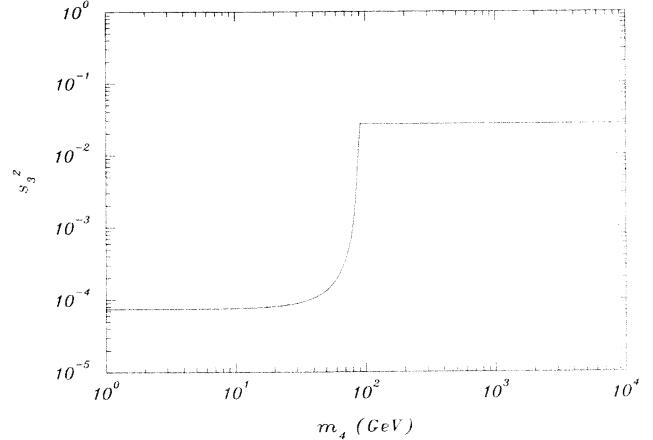


FIG. 1. The 90% C.L. upper bound of $s_3^2$ as a function of $m_4$ obtained from the $Z$ decay.

scheme [10], the precisely measured quantity $m_W/m_Z$ can be related to $G_F$ in the following way:

$$1 - \frac{m_W^2}{m_Z^2} = \frac{A_0^2}{m_w} \left[1 - |\mathcal{O}_{e4}|^2\right]^{1/2} \left[1 - |\mathcal{O}_{\mu4}|^2\right]^{1/2} \frac{1}{1 - \Delta r} , \tag{3.5}$$

where $A_0^2 = \pi\alpha_{em}/\sqrt{2}/G_F = (37.2803 \text{ GeV})^2$. The quantity $\Delta r$ depends on the masses of the top quark and Higgs boson. Taking 100 GeV $\leq m_H \leq 1$ TeV and 100 GeV $\leq m_t \leq 200$ GeV, we find $1.87 \times 10^{-2} \leq \Delta r \leq 6.77 \times 10^{-2}$ [10]. Using the experimental value given by Langacker in Ref. [8], we obtain

$$\left[1 - |\mathcal{O}_{e4}|^2\right]\left[1 - |\mathcal{O}_{\mu4}|^2\right] \geq (0.9436)^2 , \tag{3.6}$$

at 90% C.L., leading to an upper bound for $|\mathcal{O}_{e4}|^2|\mathcal{O}_{\mu4}|^2$ given by

$$|\mathcal{O}_{e4}|^2|\mathcal{O}_{\mu4}|^2 \leq 3.18 \times 10^{-3} , \tag{3.7}$$

or $s_3{}^2 \leq 0.11$ which is much less stringent than using the neutrino counting in $Z$ decay as given in Eq. (3.2). In other words, the presence of a right-handed neutrino does not play an important role for the precision measurement of $m_W/m_Z$.

The presence of a right-handed neutrino does violate the $\mu$-$e$ universality in charged current processes. Let us first consider the classic violation of the generation universality test in pion decay. The ratio of the decay rates $R = \Gamma(\pi \to e\nu)/\Gamma(\pi \to \mu\nu)$ in the presence of neutrino mixings is given by

$$R = \frac{\Gamma(\pi \to e\nu)}{\Gamma(\pi \to \mu\nu)} = R_0 \frac{1 - |\mathcal{O}_{e4}|^2}{1 - |\mathcal{O}_{\mu4}|^2} . \tag{3.8}$$

The experimental measurement relative to the standard model expectation, $R/R_0$, was recently calculated to be $0.9969 \pm 0.0031 \pm 0.004$ [11], yielding

PHENOMENOLOGICAL CONSEQUENCES OF SINGLET NEUTRINOS

$$\frac{1 - |\mathcal{O}_{e4}|^2}{1 - |\mathcal{O}_{\mu 4}|^2} = 0.9969 \pm 0.0051. \tag{3.9}$$

Next, we consider the charged current processes involving quarks, where the Cabibbo-Kobayashi-Maskawa (CKM) matrix $(V)$ relevant for nuclear $\beta$ and $K_{e3}$ decays is now modified by

$$|\tilde{V}_{ud}|^2 = \frac{|V_{ud}|^2}{1 - |\mathcal{O}_{\mu 4}|^2} \,, \quad |\tilde{V}_{us}|^2 = \frac{|V_{us}|^2}{1 - |\mathcal{O}_{\mu 4}|^2} \,. \tag{3.10}$$

Experimentally, the quantity $|\tilde{V}_{ud}|^2 + |\tilde{V}_{us}|^2 + |\tilde{V}_{ub}|^2$ is measured to be $0.9981 \pm 0.0021$ [12]. Since $|\tilde{V}_{ub}|^2 \le (0.01)^2$, its contribution is less than the uncertainty of the measurement. Thus neglecting the contribution of $|\tilde{V}_{ub}|^2$ is well justified. Since the quark sector is not affected by the introduction of singlet neutrinos, the unitarity of $V$ still holds, and exploiting that gives

$$|\mathcal{O}_{\mu 4}|^2 < 1.5 \times 10^{-3} \tag{3.11}$$

at 90% C.L. Combining Eqs. (3.9) and (3.11), we obtain

$$|\mathcal{O}_{e4}|^2 < 1.0 \times 10^{-2} \tag{3.12}$$

at 90% C.L.

As with the invisible decay width of $Z$, the presence of right-handed neutrinos will increase the lifetime of the $\tau$. The updated world averages of the $\tau$ lepton mass and lifetime are given by $m_\tau = 1770.0 \pm 0.4$ MeV and $\tau_\tau = 295.9 \pm 10^{-15}$ s, respectively, and the relevant leptonic branching ratios are $B(\tau \to e\nu\nu) = 17.77 \pm 0.15\%$ and $B(\tau \to \mu\nu\nu) = 17.48 \pm 0.18\%$, as discussed in Ref. [13]. Using these values for $m_\tau$ and $\tau_\tau$, the theoretical expectations for the branching ratios are $B(\tau \to e\nu\nu)|_{\text{theor}} = 18.13 \pm 0.20\%$ and $B(\tau \to \mu\nu\nu)|_{\text{theor}} = 17.63 \pm 0.20\%$ [14]. We can see that the experimental values for the branching ratios are smaller than the theoretical expectation. If the right-handed neutrino is responsible for the discrepancies, we obtain

$$\frac{B(\tau \to e\nu\nu)}{B(\tau \to e\nu\nu)|_{\text{theor}}} + \frac{B(\tau \to \mu\nu\nu)}{B(\tau \to \mu\nu\nu)|_{\text{theor}}}$$
$$= \left[1 - |\mathcal{O}_{\tau 4}|^2\right]\left[2 - |\mathcal{O}_{e4}|^2 - |\mathcal{O}_{\mu 4}|^2\right]$$
$$= 1.9716 \pm 0.0204 \,. \tag{3.13}$$

At 90% C.L., this translates into limits on $c_2$ and $s_3$ as

$$s_3^2(1 + c_2^2) \le 6.1 \times 10^{-2} \,, \tag{3.14}$$

or $s_3^2 \le 6.1 \times 10^{-2}$ which is again less stringent than Eq. (3.2).

## IV. LEPTON-NUMBER-VIOLATING PROCESSES

In this section, we compute, in the Feynman gauge, rare lepton-number-violating (LNV) decay processes of the muon to one-loop accuracy. To a very good approx-

imation, we may take the masses of $\nu_1$, $\nu_2$, and $\nu_3$ to be zero. The rare processes we are interested in are $\mu \to e\gamma$, $\mu \to 3e$, $e$-$\mu$ conversion in nuclei, and neutrinoless double-$\beta$ decay, $(2\beta)_{0\nu}$. Details of the calculation of one-loop diagrams are given in Appendix B.

Before going into the rare decay processes, we first consider the large $m_4$ behavior of LNV penguin diagrams, $\mu$-$e$-$Z$ and $\mu$-$e$-$\gamma$, and the two-$W$ box diagrams given in Figs. 2, 3, and 4. Generic properties of the decoupling effect for the seesaw model have been considered recently in Ref. [15]. Here, we treat $s_3$ as an independent parameter, and consider the asymptotic behavior of the lepton-flavor-violating effective vertices as $m_4$ goes to infinity.

Let us begin with the the photon penguin diagrams shown in Fig. 2. For large $m_4$, the effective vertices of the photonic penguin diagram, Eqs. (B2) and (B3), are given by

$$\lim_{x_4 \to \infty} F_1 = s_1 c_1 s_2^2 s_3^2 \left(-\frac{\ln x_4}{6}\right) \,, \tag{4.1}$$

$$\lim_{x_4 \to \infty} F_2 = s_1 c_1 s_2^2 s_3^2 \left(-\frac{1}{2}\right) \,. \tag{4.2}$$

The decoupling theorem is violated for both $F_1$ and $F_2$.

For the $Z$ penguin diagrams shown in Fig. 3, the effective vertex given by Eq. (B16) for $x_4$ large becomes

$$\lim_{x_4 \to \infty} P_Z = s_1 c_1 s_2^2 s_3^2 \left(s_3^2 \frac{x_4}{4} \ln x_4\right) \,, \tag{4.3}$$

where this term comes from the Majorana nature of $\nu_4$. Hence, we can see that the decoupling theorem is also violated for the $Z$ penguin.

Finally, we consider the box diagram for $\mu \to 3e$, shown in Fig. 4. When $x_4$ is large, $B_{\mu \to 3e}$ from Eq. (B25) becomes



(a)   (b)

(c)   (d)

(e)   (f)
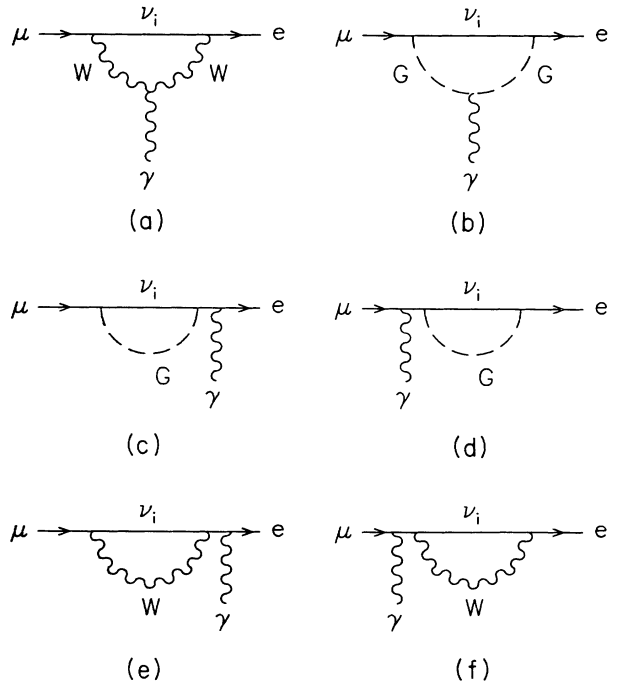
FIG. 2. Photon penguin diagrams for the $\mu$-$e$-$\gamma$ vertex.

$$\lim_{x_4 \to \infty} B_{\mu \to 3e} = s_1 c_1 s_2^2 s_3^2 \left( s_1^2 s_2^2 s_3^2 \frac{x_4}{2} \ln x_4 \right) , \qquad (4.4)$$

where this term comes from the diagrams in Figs. 4(e,f,g,h). Again, the decoupling theorem is violated.

We now consider each of these processes in some detail.

(a) $\mu \to e\gamma$. The transition amplitude for the process $\mu \to e\gamma$ is given by

$$\text{Amp}(\mu \to e\gamma)$$
$$= \frac{g^2 e}{32\pi^2 m_W^2} F_2 \, \epsilon^\mu(q) \, \bar{e} \, i\sigma_{\mu\nu} q^\nu m_\mu \frac{1 + \gamma_5}{2} \mu , \quad (4.5)$$

where $\epsilon^\mu(q)$ is the polarization vector of the photon with outgoing momentum $q$. Hence, the decay branching ratio is given by

$$B(\mu \to e\gamma) = \frac{3\alpha}{2\pi} |F_2|^2 . \qquad (4.6)$$

(b) $\mu \to 3e$. This process involves the photon and $Z$ penguin as well as box diagrams. The interaction Lagrangian is given by

$$\mathcal{L}(\mu \to 3e) = -\frac{\alpha G_F}{\sqrt{2}\pi} \left\{ F_2 \, \bar{e} \, \gamma^\mu \, e \, \bar{e} \, i\frac{\sigma_{\mu\nu} q^\nu}{q^2} m_\mu \frac{1 + \gamma_5}{2} \mu + \bar{e} \, \gamma^\mu \left[ L\frac{1 - \gamma_5}{2} + R\frac{1 + \gamma_5}{2} \right] e \, \bar{e} \, \gamma_\mu \frac{1 - \gamma_5}{2} \mu \right\} , \qquad (4.7)$$

where $L$ and $R$ are defined as

$$L = F_1 + \frac{1}{s_W^2} \left( -\frac{1}{2} + s_W^2 \right) P_Z - \frac{1}{2s_W^2} B_{\mu \to 3e} , \qquad (4.8)$$
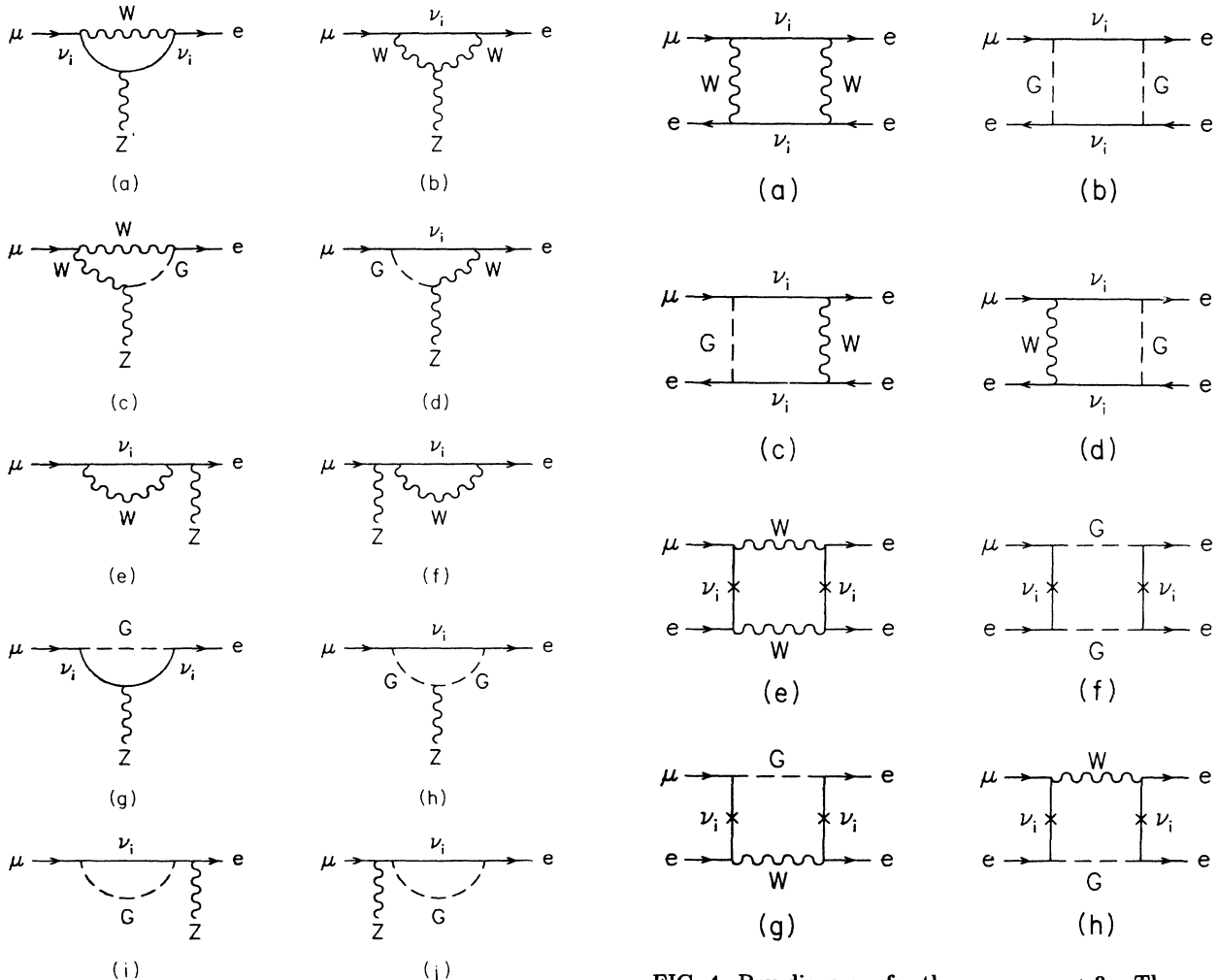
FIG. 3. $Z$ penguin diagrams for the $\mu$-$e$-$Z$ vertex.

FIG. 4. Box diagrams for the process $\mu \to 3e$. The crosses correspond to flipping the neutrino helicities.

$$R = F_1 + P_Z \ . \tag{4.9}$$

Hence, we obtain the branching ratio which is given by

$$B(\mu \to 3e) = \frac{\alpha^2}{16\pi^2} \left\{ R^2 + 2L^2 - 4F_2(R+2L) + 4F_2^2 \left( 4\ln\frac{m_\mu}{2m_e} - \frac{13}{6} \right) \right\} \ . \tag{4.10}$$

(c) $\mu$-$e$ conversion in nuclei. The Feynman diagrams for this process can be obtained from that of $\mu \to 3e$ by replacing the electron lines by quark lines. Hence, the interaction Lagrangian is given by

$$\mathcal{L}(\mu\text{-}e) = -\frac{\alpha G_F}{\sqrt{2}\pi} \left\{ \bar{e} \ i\frac{\sigma_{\mu\nu}q^\nu}{q^2} \ m_\mu \frac{1+\gamma_5}{2} \ \mu \left[ -\frac{2}{3}F_2 \ \bar{u} \ \gamma^\mu \ u + \frac{1}{3}F_2 \ \bar{d} \ \gamma^\mu \ d \right] + \bar{e} \ \gamma_\mu \frac{1-\gamma_5}{2} \ \mu \sum_{q=u,d} V_q \ \bar{q} \ \gamma_\mu \ q \right\} \ , \tag{4.11}$$

where the $V_q$'s are defined by

$$V_u = -\frac{2}{3}F_1 + \frac{1}{s_W^2} \left( \frac{1}{4} - \frac{2}{3}s_W^2 \right) P_Z - \frac{1}{4s_W^2}B_{\mu\text{-}e}^u \ , \tag{4.12}$$

$$V_d = \frac{1}{3}F_1 + \frac{1}{s_W^2} \left( -\frac{1}{4} + \frac{1}{3}s_W^2 \right) P_Z - \frac{1}{4s_W^2}B_{\mu\text{-}e}^d \ . \tag{4.13}$$

In the above, we include only the vector part of the quark current because its contribution is larger than that of the axial vector part due to the nuclear coherent effect [16]. Following the standard procedure [17–19], we obtain the transition rate for the $\mu$-$e$ conversion in nuclei as follows:

$$\Gamma(\mu N \to eN) = \frac{\alpha^5 G_F^2 m_\mu^5}{16\pi^4} \frac{Z_{\text{eff}}^4}{Z} |F(-m_\mu^2)|^2 |Q_W|^2 \ , \tag{4.14}$$

with

$$Q_W = \left( \frac{2}{3}F_2 + V_u \right)(2Z+N)$$
$$+ \left( -\frac{1}{3}F_2 + V_d \right)(Z+2N) \ , \tag{4.15}$$

where $Z$ and $N$ are the atomic (or proton) and neutron numbers for the nuclei, and $|F(-m_\mu^2)|$ and $Z_{\text{eff}}$ are the nuclear form factor and the effective atomic number. For $^{48}_{22}$Ti, one has $|F(-m_\mu^2)| = 0.54$ [20] and $Z_{\text{eff}} = 17.6$ [21].

From the present data, the branching ratios $B(\mu \to e\gamma)$, $B(\mu \to 3e)$ and $B(\mu \ \text{Ti} \to e \ \text{Ti}) = \Gamma(\mu \ \text{Ti} \to e \ \text{Ti})/\Gamma(\mu \ \text{capture})$ are $4.9 \times 10^{-11}$ [22], $1.0 \times 10^{-12}$ [23], and $4.6 \times 10^{-12}$ [24], respectively, which translate into

$$|F_2|^2 \leq 1.4 \times 10^{-8} \ , \tag{4.16}$$

$$\left[ R^2 + 2L^2 - 4F_2(R+2L) + 65.0F_2^2 \right] \leq 3.0 \times 10^{-6} \ , \tag{4.17}$$

$$\left[ 70 \left( \frac{2}{3}F_2 + V_u \right) + 74 \left( -\frac{1}{3}F_2 + V_d \right) \right]^2 \leq 2.6 \times 10^{-4} \ , \tag{4.18}$$

respectively. Note that the constraints, Eqs. (4.16), (4.17), and (4.18) are independent of models.

At the first sight, it would seem that $\mu \to e\gamma$ provides the most stringent constraint among all three processes. To compare among the experiments, let us consider the ratios

$$S_1 = \frac{B(\mu \to 3e)}{B(\mu \to e\gamma)} \frac{4.9 \times 10^{-11}}{1.0 \times 10^{-12}} \tag{4.19}$$

and

$$S_2 = \frac{B(\mu \ \text{Ti} \to e \ \text{Ti})}{B(\mu \to e\gamma)} \frac{4.9 \times 10^{-11}}{4.6 \times 10^{-12}} \ , \tag{4.20}$$

which provide a measure of the sensitivity of experiments. For simplicity, we first neglect the contributions of the last terms in Eqs. (B16) and (B25). Hence the ratios become independent of $\mathcal{O}$. It can be easily shown that the ratios $S_{1,2}$ are generically given by $(\ln x_4)^2$ for small and large $x_4$ owing to the $Z$ penguin diagrams. Thus, experiments $\mu \to 3e$ and $\mu$-$e$ conversion have advantages over $\mu \to e\gamma$ in probing singlet Majorana neutrinos. We plot the ratios as functions of $m_4$ in Fig. 5. Furthermore, $\mu$-$e$ conversion is further enhanced by the coherence of the nuclei. Therefore, we can use Eq. (4.18), which is obtained from $\mu$-$e$ conversion in nuclei, to place an upper bound on the mass of $\nu_4$ as a function of $|\mathcal{O}_{\mu 4}^* \mathcal{O}_{e4}|$. In
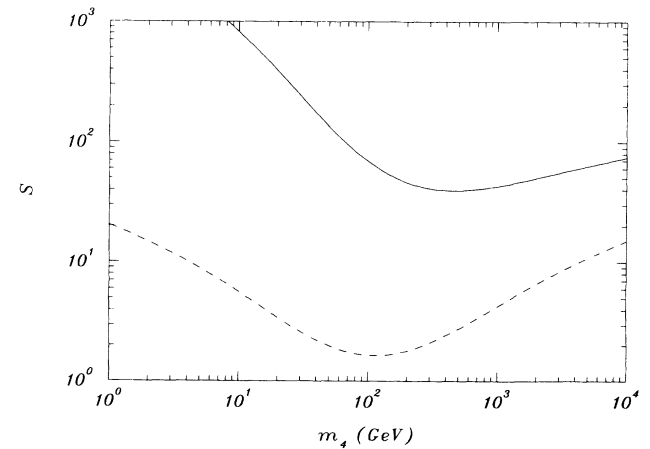


FIG. 5. Sensitivity ($S$) of experiments, $\mu \to 3e$ (dashed line) and $\mu$-$e$ conversion (solid line), relative to $\mu \to e\gamma$, where $S = S_1$ and $S_2$, respectively.

general, Eq. (4.18) depends on $s_3$ and $|\mathcal{O}_{e4}|$. Hence, we vary the values, within the allowed range given in Fig. 1, to obtain stronger and weaker bounds on $m_4$. The result is depicted in Fig. 6. In particular, for $m_4 \geq m_W$, the stronger bound is given by the maximally allowed value of $s_3$ whereas the weaker bound is given by $s_3 = 0$.

## V. NEUTRINOLESS DOUBLE-$\beta$ DECAY

The classic process to test for the Majorana nature of neutrino masses is neutrinoless double-$\beta$ decay, as depicted in Fig. 7. The effective Lagrangian is given by

$$\mathcal{L}_{\beta\beta0\nu} = G_F^2 \frac{1}{q^2} \left[ \sum_{i=1}^{4} \mathcal{O}_{ei}^2 m_i \frac{q^2}{q^2 - m_i^2} \right] \bar{e} \, \gamma^\mu \gamma^\nu (1 + \gamma_5) \, e^c \, \bar{u} \, \gamma_\mu (1 - \gamma_5) \, d \, \bar{u} \, \gamma_\nu (1 - \gamma_5) \, d \, , \tag{5.1}$$

where $q$ is the momentum carried by the internal neutrino line. After integrating over all possible intermediate nuclear states, the quantity in the square brackets in Eq. (5.1) becomes

$$m_\nu(\text{eff}) = \sum_{i=1}^{4} \mathcal{O}_{ei}^2 m_i \, F(m_i, A) \tag{5.2}$$

and [25]

$$F(m, A) = \left\langle \frac{e^{-mr}}{r} \right\rangle \Big/ \left\langle \frac{1}{r} \right\rangle , \tag{5.3}$$

where $A$ is the total number of the nucleon. Using the approximation of a uniform two-nucleon correlation of a hard core ($r_c = 0.5$ fm) [26], Eq. (5.3) becomes

$$F(m, A) = \frac{0.5}{(mR)^2} [(1 + mr_c)e^{-mr_c} - (1 + 2mR)e^{-2mR}], \tag{5.4}$$

where $R$ is the nuclear radius which is taken to be $R = 1.2A^{1/3}$ fm. Notice that if neutrinos have opposite $CP$, there will be a cancellation between their contributions.

In particular, if both $m_3$ and $m_4$ are light, $F(m_{3,4}, A)$ would be approximately equal to unity. Hence, Eq. (5.2) is then equal to $s_1^2 s_2^2 (-c_3^2 m_3 + s_3^2 m_4)$ which would be zero if we restrict ourselves to the seesaw mixing relation, Eq. (2.8). The cancellation is not complete when one includes the nuclear correlation, Eq. (5.3). Again, here we consider a general case where $s_3$ is considered as an independent parameter.

The best experimental limit on the quantity $|m_\nu(\text{eff})|$ is 1.5 eV [27], which translates into

$$s_1^2 s_2^2 | - c_3^2 \, m_3 \, F(m_3, A) + s_3^2 \, m_4 \, F(m_4, A)| \leq 1.5 \text{ eV} . \tag{5.5}$$

Let us first consider the contribution from $\nu_4$. Numerically, we have $s_3^2 \, m_4 \, F(m_4, A) \leq 1.6 \times 10^{-8}$ ($1.2 \times 10^{-10}$) GeV for $m_4 = 1$ (2.5) GeV, where $s_3$ is taken to be the maximally allowed value shown in Fig. 1. Therefore, one would expect the $\nu_3$ contribution to be important, leading to

$$s_1^2 s_2^2 \leq \frac{1.5 \text{ eV}}{m_3}. \tag{5.6}$$

As a result, $s_1 s_2$ would be very small when $\nu_3$ is relatively heavy. In particular, if $m_3 = 1$ MeV, we obtain $s_1 s_2 < 10^{-3}$.

## VI. NEUTRINO OSCILLATIONS

In the scenario we are considering, there are two massive and two massless neutrinos; oscillation [28,29] of neutrino flavors will be allowed, leading to interesting phe-

FIG. 6. The stronger (solid line) and weaker (dashed line) upper bounds on $m_4$ derived from the $\mu$-$e$ conversion experiment as a function of $|\mathcal{O}_{\mu4}^* \mathcal{O}_{e4}|$, where we have included the bound obtained from $Z$ decays.
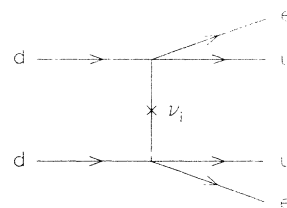
FIG. 7. The mechanism for neutrinoless double-$\beta$ decay, where the cross corresponds to flipping the neutrino helicity.

nomena not available in the standard model. When the mass of $\nu_4$ is greater than the neutrino beam energy, there will be three-flavor oscillation with one oscillation wavelength, $\lambda_3 = 4\pi E/m_3^2$. In addition, when we assume $s_3$ to be very small, the oscillation mechanism depends only on two mixings, namely, $s_1$, and $s_2$. Hence, for this situation the parameters required to describe neutrino oscillations are just $\lambda_3$, $s_1$ and $s_2$.

Let us first consider the neutrino-neutrino oscillation probabilities. The oscillation probabilities corresponding to an electron neutrino $(\nu_e)$, which travels a distance $L$, are given by

$$P(\nu_e \to \nu_e) = 1 - 4\sin^2(\tfrac{1}{2}k_3L)\left(s_1^2 s_2^2 - s_1^4 s_2^4\right), \quad (6.1)$$

$$P(\nu_e \to \nu_\mu) = 4\sin^2(\tfrac{1}{2}k_3L)\left(s_1^2 s_2^4 - s_1^4 s_2^4\right), \quad (6.2)$$

$$P(\nu_e \to \nu_\tau) = 4\sin^2(\tfrac{1}{2}k_3L)\left(s_1^2 s_2^2 - s_1^2 s_2^4\right), \quad (6.3)$$

where

$$k_3 = \frac{2\pi}{\lambda_3} = 2.5m^{-1}\frac{m_3^2 \text{ (eV)}}{2E \text{ (MeV)}}. \quad (6.4)$$

When $m_3$ is in the MeV range, the mixing $s_1^2 s_2^2$ is constrained to be $10^{-6}$ or less, Eq. (5.6). Hence, the oscillation becomes purely academic. Furthermore, neutrino and antineutrino oscillations, such as $\nu_e$-$\bar{\nu}_\tau$, are also allowed. However, it would be either suppressed by the ratio $m_3/E$ or by small mixings, Eq. (5.6), if $m_3 \gg 1$ eV.

We next consider the case when $m_3$ is small. We will consider the following three cases:

$k_3L \ll 1$. When the neutrino source is very close to the target, i.e., $L \ll 1/k_3$, the oscillation effects are small. Hence, the probability $P(\nu_\mu \to \nu_e)$ given by $|\mathcal{O}_{\mu 4}|^2|\mathcal{O}_{e4}|^2$, which is stringently constrained from $\mu$-$e$ conversion experiment, would be in the order of $10^{-8}$. Hence, lepton-number-violating scatterings, such as $\nu_\mu N \to eN'$, are negligible.

$k_3L \sim 1$. In this case, there will be oscillations. In particular, the recent accelerator experment [30] allows us to probe $m_3$ in the range 0.1–10 eV. For atmospheric neutrino experiments, the mass range of $10^{-3}$–$10^{-1}$ eV would be probed. Constraints on three neutrino mixings from atmospheric and reactor data have been studied [31] for $m_1 = m_2 = 0$ and $m_3 > 0$.

$k_3L \gg 1$. In this case, the oscillation effect is averaged out, namely, $\langle\sin^2(\tfrac{1}{2}k_3L)\rangle = 1/2$. In particular, the recent GALLEX experiment, $P(\nu_e \to \nu_e) = 0.66 \pm 0.12$, limits $s_1^2 s_2^2$ to be within either in the region of $0.64 \leq s_1^2 s_2^2 \leq 0.87$ or $0.13 \leq s_1^2 s_2^2 \leq 0.36$ at the $1\sigma$ level.

Therefore, even if $s_3$ turns out to be very small, neutrinoless double-$\beta$ decay and neutrino oscillation experiments provide more important information for this model.

## VII. CONCLUSION

In this paper, we have studied the phenomenology of having right-handed neutrino isosinglets. In principle, when there is more than one right-handed neutrino, the masses of the light neutrinos are not necessary given by $m_D^2/M$, where $m_D$ and $M$ are the Dirac and Majorana mass terms. In this paper, we regard the right-handed neutrino $\nu^c$ as an effective collection of an arbitrary number of neutrinos and allow the mixing $s_3$ to be an independent parameter rather than restricted by the seesaw relationships.

In the presence of $\nu^c$, nondiagonal neutrino $Z$ coupling exists at the tree level. When $\nu_4$ is lighter than $Z$, the decays $Z \to \nu_3 \nu_4$ and $Z \to \nu_4 \nu_4$ are allowed. Hence, the decays of $\nu_4$ would give rise to exotic $Z$ decays, such as $Z \to e \mu + X$. Including the recent search for the lepton flavor violation in $Z$ decay, we plot the result in Fig. 1. Furthermore, the violations of universalities in charged current processes are also considered, and the constraints on $\mathcal{O}_{e4}$ and $\mathcal{O}_{\mu 4}$ are $1.0 \times 10^{-2}$ and $1.5 \times 10^{-3}$, respectively. $\tau$ decays do not provide stringent constraints in this context.

Owing to the mixing and explicit Majorana mass term for $\nu^c$, both separate and total lepton numbers are not conserved. This allows rare muon decays and neutrinoless double-$\beta$ decays. Among various rare muon decay processes, $\mu$-$e$ conversion in nuclei places the most severe constraints on the model. Including the constraints derived from $Z$ decays, we plot the upper bounds of $m_4$ as a function of $|\mathcal{O}_{\mu 4}^* \mathcal{O}_{e4}|$ in Fig. 6.

For the neutrinoless double-$\beta$ decay, the contribution coming from $\nu_3$ is more important, leading to the constraint $s_1^2 s_2^2 \leq 1.5$ eV/$m_3$. In this model, three-flavor oscillation depends only on one oscillation wavelength and two mixing angles. Thus, constraints from neutrino double-$\beta$ decay as well as the solar and atmospheric neutrino experiments provide more important information for the model.

*Note added.* We are grateful to our colleagues for pointing out previous work on lepton nonuniversality in $Z$ decays [33] in the same model, and rare muon decays [34] in other models with new fermion masses much lighter than the $W$ boson mass.

## APPENDIX A: CONDITIONS OBVIATING THE SEESAW MIXING RELATIONSHIP

The most general mass matrix for $n$ generations of left-handed and $m$ generations of right-handed neutrinos takes the form

$$\begin{pmatrix} 0 & \cdots & 0 & x_{11} & \cdots & x_{1m} \\ \vdots & \ddots & \vdots & \vdots & \ddots & \vdots \\ 0 & \cdots & 0 & x_{n1} & \cdots & x_{nm} \\ x_{11} & \cdots & x_{n1} & M_{11} & \cdots & M_{1m} \\ \vdots & \ddots & \vdots & \vdots & \ddots & \vdots \\ x_{1m} & \cdots & x_{nm} & M_{m1} & \cdots & M_{mm} \end{pmatrix} . \qquad (A1)$$

We restrict our attention to the case $n \geq m$, and assume that there is only an isodoublet Higgs field so that Majorana masses for left-handed neutrinos are zero. The quantities $x_{i\alpha}$ are Dirac masses, and are given by the product of the Yukawa coupling constants and the vacuum expectation value of the isodoublet Higgs field. The $m \times m$ matrix $M_{ij}$ is the Majorana masses for the right-handed neutrinos.

Without loss of generality, we may assume that the $M_{ij}$ matrix is diagonal. Next, we regard the vectors $\mathbf{x}_i$ with $i = 1, ..., m$, vectors in $n$-dimensional flavor space, and subject the neutrinos to a rotation in this space. By this means, it will be possible to reduce $n$-$m$ of these vectors to a form where their first $n$-$m$ components are zero. Hence, $n$-$m$ neutrinos will be decoupled from massive neutrinos, and remain massless at the tree level.

For example, take the case of three generations of left-handed and two generations of right-handed neutrinos. The Yukawa couplings define for us two vectors in three-dimensional space. By the above argument, we can project out the massless neutrino, leading to the resultant mass matrix

$$\begin{pmatrix} 0 & 0 & x_{21} & x_{22} \\ 0 & 0 & x_{31} & x_{32} \\ x_{21} & x_{31} & M_1 & 0 \\ x_{22} & x_{32} & 0 & M_2 \end{pmatrix} . \qquad (A2)$$

The determinant of this mass matrix is given by $(\mathbf{x}_1 \times$

$\mathbf{x}_2)^2$. For large $M_{1,2}$, and generic values for $\mathbf{x}_{1,2}$, there will be two light and two heavy neutrinos. The masses of the light neutrinos are given by the seesaw mass relationships of the form $m_\nu \sim \mathbf{x}_1 \times \mathbf{x}_2/M$, when $M$ is the collective mass for $M_{1,2}$. In addition, the mixings of the light and heavy neutrino are of order $x/M = \sqrt{m_\nu/M}$, where $x$ is a generic component of $\mathbf{x}_{1,2}$. From solar and atmospheric neutrino experiments, $m_\nu$ is required to be of order $10^{-3}$ eV. If we take $M$ to be $10^{15}$ $(10^2)$ GeV, then from the seesaw mass relationship $x$ will be of order $10^2$ $(10^{-5})$ GeV. As a result, the mixing $x/M$ would be very small, leading to negligible exotic processes such as $\mu \to e\gamma$, $\mu \to 3e$, and $\mu$-$e$ conversion in nuclei.

To enhance the mixing, one must evade the seesaw mass relationships. For example, when $\mathbf{x}_1 \times \mathbf{x}_2 \sim 0$, one of the two light neutrinos will become massless. In addition, when $M_1\mathbf{x}_2^2 + M_2\mathbf{x}_1^2 \sim 0$, the remaining light neutrino will also become massless. Now, the mixing, which is still given as $x/M$, cannot be rewritten as the ratio of light to heavy neutrino masses. Such apparently geometric conditions could be remnants of a symmetry manifested only at higher energies. In the phenomenological analysis described in this paper, we consider such possibilities by allowing the mixing to be an independent parameter.

## APPENDIX B: ONE-LOOP DIAGRAM CALCULATION

### 1. Photon penguin

The calculation is identical to that of sequential lepton models. The effective vertex of diagrams shown in Fig. 2 is given by

$$\Gamma_\mu^\gamma = \frac{g^2 e}{32\pi^2 m_W^2} \left[ F_1 \left( q^2 \gamma_\mu - \slashed{q}q_\mu \right) \bar{e} \frac{1 - \gamma_5}{2} \mu + F_2 \bar{e} \, i\sigma_{\mu\nu}q^\nu \, m_\mu \frac{1 + \gamma_5}{2} \mu \right] , \qquad (B1)$$

where [32]

$$F_1 = \mathcal{O}_{\mu 4}^* \mathcal{O}_{e4} \left[ \frac{x_4(12 + x_4 - 7x_4^2)}{12(x_4 - 1)^3} + \frac{x_4^2(-12 + 10x_4 - x_4^2)}{6(x_4 - 1)^4} \ln x_4 \right] , \qquad (B2)$$

$$F_2 = \mathcal{O}_{\mu 4}^* \mathcal{O}_{e4} \left[ \frac{x_4(1 - 5x_4 - 2x_4^2)}{4(x_4 - 1)^3} + \frac{3x_4^3}{2(x_4 - 1)^4} \ln x_4 \right] , \qquad (B3)$$

where $x_4 = m_4^2/m_W^2$. It can be easily checked that the contribution of $x_4$ is much larger than that of $x_3$ for $x_3 \ll 1$ and $x_3 \ll x_4$. For $x_3$, $x_4 \ll 1$, the muon-number-violating processes would be too small to be experimentally interesting. Hence, within the parameter space we are considering in this paper, we can simply neglect the contribution of $x_3$.

### 2. $Z$ penguin

$Z$ penguin diagrams depicted in Fig. 3 are more complicated than the photon penguin because of the nondiagonal coupling [see Eqs. (2.13) and (2.19)], as well as the Majorana nature of neutrinos. The $Z\bar{e}\mu$ effective vertex is defined as

$$\Gamma_\mu^Z = \frac{g^3}{32\pi^2 \cos\theta_W} \sum_\alpha \Gamma_\alpha \; \bar{e} \; \gamma_\mu \frac{1-\gamma_5}{2} \mu \; , \qquad \text{(B4)}$$

where the calculation of each diagram is given by

$$\Gamma_a = \sum_{i=1}^{4} \mathcal{O}_{\mu i}^* \mathcal{O}_{ei} \left[ \frac{1}{\varepsilon} - \frac{3}{4} + \frac{1}{2} F(x_i, x_i) + x_i G(x_i, x_i) \right]$$

$$- \sum_{i,j=1}^{4} \mathcal{O}_{\mu j}^* \mathcal{O}_{ei} \mathcal{O}_{Ri}^* \mathcal{O}_{Rj} \left[ \frac{1}{\varepsilon} - \frac{3}{4} + \frac{1}{2} F(x_i, x_j) \right]$$

$$- \sum_{i,j=1}^{4} \mathcal{O}_{\mu j}^* \mathcal{O}_{ei} \mathcal{O}_{Ri} \mathcal{O}_{Rj}^* \left[ \sqrt{x_i x_j} G(x_i, x_j) \right] \; ,$$

$$\text{(B5)}$$

$$\Gamma_b = \sum_{i=1}^{4} \mathcal{O}_{\mu i}^* \mathcal{O}_{ei} (1 - s_W^2) \left[ -\frac{6}{\varepsilon} + \frac{1}{2} - 3F(x_i, x_j) \right] \; ,$$

$$\text{(B6)}$$

$$\Gamma_{c+d} = \sum_{i=1}^{4} \mathcal{O}_{\mu i}^* \mathcal{O}_{ei} s_W^2 \left[ -2x_i G(1, x_i) \right] \; , \qquad \text{(B7)}$$

$$\Gamma_{e+f} = \sum_{i=1}^{4} \mathcal{O}_{\mu i}^* \mathcal{O}_{ei} \left( \frac{1}{2} - s_W^2 \right) [F(1, x_i)] \; , \qquad \text{(B8)}$$

$$\Gamma_g = \sum_{i=1}^{4} \mathcal{O}_{\mu i}^* \mathcal{O}_{ei} \left[ -\frac{1}{2} x_i^2 G(x_i, x_i) - \frac{1}{4} x_i F(x_i, x_i) \right]$$

$$+ \sum_{i,j=1}^{4} \mathcal{O}_{\mu j}^* \mathcal{O}_{ei} \mathcal{O}_{Ri}^* \mathcal{O}_{Rj} \left[ \frac{1}{2} x_i x_j G(x_i, x_j) \right]$$

$$+ \sum_{i,j=1}^{4} \mathcal{O}_{\mu j}^* \mathcal{O}_{ei} \mathcal{O}_{Ri} \mathcal{O}_{Rj}^* \left[ \frac{1}{4} \sqrt{x_i x_j} F(x_i, x_j) \right] \; , \quad \text{(B9)}$$

$$\Gamma_h = \sum_{i=1}^{4} \mathcal{O}_{\mu i}^* \mathcal{O}_{ei} (\frac{1}{2} - s_W^2) x_i \left[ -\frac{1}{\varepsilon} - \frac{1}{4} - \frac{1}{2} x_i G(1, x_i) \right] \; ,$$

$$\text{(B10)}$$

$$\Gamma_{i+j} = -\Gamma_h \qquad \text{(B11)}$$

with

$$F(a, b) = 1 - \frac{a^2}{(a-1)(a-b)} \ln a - \frac{b^2}{(b-1)(b-a)} \ln b \; ,$$

$$\text{(B12)}$$

$$G(a, b) = -\frac{a}{(a-1)(a-b)} \ln a - \frac{b}{(b-1)(b-a)} \ln b \; .$$

$$\text{(B13)}$$

Each of the divergent diagrams in Figs. 3(a–f) is finite after summing all the internal neutrinos due to the unitarity of $\mathcal{O}$ and Eq. (2.5); the divergences cancel among diagrams in Figs. 3(g–j). Note that dependence on $s_W^2$ disappears when all the diagrams are summed because of gauge invariance. The last terms in the first lines of Eqs. (B5) and (B9) are due to the Majorana property of neutrinos, the second lines there are due to nondiagonal neutrino-$Z$ couplings, and the last lines are due to both properties. Summing over all contributions, we obtain

$$\sum_\alpha \Gamma_\alpha = \sum_{i=3}^{4} \mathcal{O}_{\mu i}^* \mathcal{O}_{ei} \left[ \left( \frac{x_i^2 - 6x_i}{2(x_i - 1)} + \frac{3x_i^2 + 2x_i}{2(x_i - 1)^2} \ln x_i \right) + \left( -\frac{3x_i}{4(x_i - 1)} + \frac{x_i^3 - 2x_i^2 + 4x_i}{4(x_i - 1)^2} \ln x_i \right) \right]$$

$$+ \sum_{i,j=3}^{4} \mathcal{O}_{\mu j}^* \mathcal{O}_{ei} \left\{ \mathcal{O}_{Ri}^* \mathcal{O}_{Rj} \left[ -\frac{x_i x_j}{2(x_i - x_j)} \ln x_i - \frac{x_j x_i}{2(x_j - x_i)} \ln x_j \right] \right.$$

$$+ \left. \mathcal{O}_{Ri} \mathcal{O}_{Rj}^* \sqrt{x_i x_j} \left[ \frac{1}{4} + \frac{4x_i - x_i^2}{4(x_i - 1)(x_i - x_j)} \ln x_i + \frac{4x_j - x_j^2}{4(x_j - 1)(x_j - x_i)} \ln x_j \right] \right\} \; . \qquad \text{(B14)}$$

Note that $|\mathcal{O}_{\mu i}^* \mathcal{O}_{Ri}| = |\mathcal{O}_{\mu i}^* \mathcal{O}_{Ri}^*| = c_1 s_2 c_3 s_3$ and $|\mathcal{O}_{ei}^* \mathcal{O}_{Ri}| = |\mathcal{O}_{ei} \mathcal{O}_{Ri}| = s_1 s_2 c_3 s_3$, for $i = 3, 4$. Hence, nondiagonal neutrino-$Z$ coupling contributions are also dominated by $x_4$, and Eq. (B14), to a very good approximation, becomes

$$P_Z = \sum_\alpha \Gamma_\alpha$$

$$= \mathcal{O}_{\mu 4}^* \mathcal{O}_{e4} \left[ \left( \frac{x_4^2 - 6x_4}{2(x_4 - 1)} + \frac{3x_4^2 + 2x_4}{2(x_4 - 1)^2} \ln x_4 \right) + \left( -\frac{3x_4}{4(x_4 - 1)} + \frac{x_4^3 - 2x_4^2 + 4x_4}{4(x_4 - 1)^2} \ln x_4 \right) \right.$$

$$+ |\mathcal{O}_{R4}|^2 \left( \frac{-2x_4^2 + 5x_4}{4(x_4 - 1)} + \frac{-x_4^3 + 2x_4^2 - 4x_4}{4(x_4 - 1)^2} \ln x_4 \right) \right] \; , \qquad \text{(B15)}$$

where the parentheses help us to identify various contributions. We can also rewrite Eq. (B15) as

$$P_Z = \mathcal{O}^*_{\mu 4} \mathcal{O}_{e4} \left[ \left( -\frac{5x_4}{2(x_4 - 1)} + \frac{2x_4 + 3x_4^2}{2(x_4 - 1)^2} \ln x_4 \right) + s_3^2 \left( \frac{2x_4^2 - 5x_4}{4(x_4 - 1)} + \frac{x_4^3 - 2x_4^2 + 4x_4}{4(x_4 - 1)^2} \ln x_4 \right) \right]. \tag{B16}$$

### 3. $\mu \to 3e$ box diagrams

There are two different classes of box diagrams, Figs. 4(a,b,c,d) and 4(e,f,g,h), which contribute to the decay of $\mu \to 3e$. The effective interaction Lagrangian is defined as

$$\frac{g^4}{64\pi^2 m_W^2} \sum_\alpha B_\alpha \, \bar{e} \, \gamma_\mu \frac{1 - \gamma_5}{2} \, e \, \bar{e} \, \gamma^\mu \frac{1 - \gamma_5}{2} \, \mu \, . \tag{B17}$$

The calculation of each diagram is given by

$$B_a = \mathcal{O}^*_{\mu 4} \mathcal{O}_{e4} \left[ \left( \frac{x_4}{x_4 - 1} - \frac{x_4}{(x_4 - 1)^2} \ln x_4 \right) + |\mathcal{O}_{e4}|^2 \left( -\frac{x_4^2 + x_4}{(x_4 - 1)^2} + \frac{2x_4^2}{(x_4 - 1)^3} \ln x_4 \right) \right], \tag{B18}$$

$$B_b = \mathcal{O}^*_{\mu 4} \mathcal{O}_{e4} |\mathcal{O}_{e4}|^2 \left[ -\frac{x_4^3 + x_4^4}{4(x_4 - 1)^2} + \frac{x_4^3}{2(x_4 - 1)^3} \ln x_4 \right], \tag{B19}$$

$$B_{c+d} = \mathcal{O}^*_{\mu 4} \mathcal{O}_{e4} |\mathcal{O}_{e4}|^2 \left[ \frac{4x_4^2}{(x_4 - 1)^2} - 2\frac{x_4^3 + x_4^4}{(x_4 - 1)^3} \ln x_4 \right], \tag{B20}$$

$$B_e = \mathcal{O}^*_{\mu 4} \mathcal{O}_{e4} |\mathcal{O}_{e4}|^2 \left[ -\frac{4x_4}{(x_4 - 1)^2} + 2\frac{x_4^2 + x_4}{(x_4 - 1)^3} \ln x_4 \right], \tag{B21}$$

$$B_f = \mathcal{O}^*_{\mu 4} \mathcal{O}_{e4} |\mathcal{O}_{e4}|^2 \left[ -\frac{x_4^3}{(x_4 - 1)^2} + \frac{x_4^4 + x_4^3}{2(x_4 - 1)^3} \ln x_4 \right], \tag{B22}$$

$$B_{g+h} = \mathcal{O}^*_{\mu 4} \mathcal{O}_{e4} |\mathcal{O}_{e4}|^2 \left[ \frac{x_4^2 + x_4}{(x_4 - 1)^2} - \frac{2x_4^2}{(x_4 - 1)^3} \ln x_4 \right], \tag{B23}$$

where the contributions from $x_3$ are negligible. Again $B_{a,b,c,d}$ are the same as the sequential lepton models, and $B_{e,f,g,h}$ are due to the Majorana properties of neutrinos. Summing up all the contributions, Eqs. (B18)–(B23), we obtain

$$
\begin{aligned}
B_{\mu \to 3e} &= \sum_\alpha B_\alpha \\
&= \mathcal{O}^*_{\mu 4} \mathcal{O}_{e4} \left[ \frac{x_4}{x_4 - 1} - \frac{x_4}{(x_4 - 1)^2} \ln x_4 + |\mathcal{O}_{e4}|^2 \left( \frac{-4x_4 + 11x_4^2 - x_4^3}{4(x - 1)^2} - \frac{3x_4^3}{2(x_4 - 1)^3} \ln x_4 \right) \right. \\
&\quad \left. + |\mathcal{O}_{e4}|^2 \left( \frac{-3x_4 + x_4^2 - x_4^3}{(x_4 - 1)^2} + \frac{4x + x^3 + x^4}{2(x_4 - 1)^3} \ln x_4 \right) \right]
\end{aligned}
\tag{B24}
$$

or

$$B_{\mu \to 3e} = \mathcal{O}^*_{\mu 4} \mathcal{O}_{e4} \left[ \frac{x_4}{x_4 - 1} - \frac{x_4}{(x_4 - 1)^2} \ln x_4 + |\mathcal{O}_{e4}|^2 \left( \frac{-16x_4 + 15x_4^2 - 5x_4^3}{4(x_4 - 1)^2} + \frac{4x - 2x^3 + x_4^4}{2(x_4 - 1)^3} \ln x_4 \right) \right]. \tag{B25}$$

### 4. $\mu\text{-}e$ conversion box diagrams

The box diagrams corresponding to $\mu\text{-}e$ conversion in nuclei can be obtained from Figs. 4(a,b,c,d) by replacing the electron lines with quark lines. The effective interactions are defined as

$$\frac{g^4}{64\pi^2 m_W^2} \bar{e} \, \gamma_\mu \frac{1 - \gamma_5}{2} \, \mu \left[ B^u_{\mu\text{-}e} \, \bar{u} \, \gamma^\mu \frac{1 - \gamma_5}{2} \, u + B^d_{\mu\text{-}e} \, \bar{d} \, \gamma^\mu \frac{1 - \gamma_5}{2} \, d \right], \tag{B26}$$

where $B^u_{\mu\text{-}e}$ and $B^d_{\mu\text{-}e}$ are given by

$$B^u_{\mu\text{-}e} = \mathcal{O}^*_{\mu 4} \mathcal{O}_{e4} \left[ \frac{4x_4}{x_4 - 1} - \frac{4x_4}{(x_4 - 1)^2} \ln x_4 \right], \tag{B27}$$

$$B_{\mu\text{-}e}^d = \mathcal{O}_{\mu 4}^* \mathcal{O}_{e4} \left[ \frac{x_4}{x_4 - 1} - \frac{x_4}{(x_4 - 1)^2} \ln x_4 \right] , \tag{B28}$$

and we have neglected the contribution from the top quark because $|V_{td}^{\text{CKM}}|^2 (m_t^2/m_W^2) \ll 1$.

[1] R. Davis, Jr., D.S. Harmer, and K.C. Hoffman, Phys. Rev. Lett. **20**, 1205 (1968); K.S. Hirata et al., ibid. **63**, 16 (1989); **65**, 1297 (1990); V.N. Gravin et al., in Proceedings of the Twenty-Fifth International Conference on High Energy Physics, Singapore, 1990, edited by K.K. Phua and Y. Yamaguchi (World Scientific, Singapore, 1991).

[2] A. Kusenko and R. Shrock, Phys. Lett. B **323**, 18 (1994).

[3] M. Gell-Mann, P. Ramond, and R. Slansky, in Supergravity, Proceedings of the Workshop, Stony Brook, New York, 1979, edited by P. van Nieuwenhuizen and D.Z. Freedman (North-Holland, Amsterdam, 1979), p. 315; T. Yanagida, in Proceedings of the Workshop on Unified Theory and Baryon Number of the Universe, Tsukuba, Japan, 1979, edited by A. Sawada and A. Sugamoto (KEK Report No. 79-18, Tsukuba, 1979).

[4] C. Jarlskog, Phys. Lett. B **241**, 579 (1990); Nucl. Phys. **A518**, 129 (1990).

[5] K.S. Babu and E. Ma, Phys. Lett. B **228**, 508 (1989).

[6] A. Bouquet and P. Salati, Nucl. Phys. **B284**, 557 (1987).

[7] C. Escobar, O. Peres, V. Pleitez, and R. Funchal, Phys. Rev. D **47**, R1747 (1993).

[8] P. Langacker, in Recent Directions in Particle Theory—From Superstrings and Black Holes to the Standard Model, Proceedings of the Theoretical Advanced Study Institute in Elementary Particle Physics, Boulder, Colorado, 1992, edited by J. Harvey and J. Polchinski (World Scientific, Singapore, 1993).

[9] L3 Collaboration, Phys. Lett. B **316**, 427 (1993).

[10] G. Degrassi, S. Fanchiotti, and A. Sirlin, Nucl. Phys. **B351**, 49 (1991).

[11] W.J. Marciano and A. Sirlin, Phys. Rev. Lett. **71**, 3629 (1993).

[12] Particle Data Group, K. Hikasa et al., Phys. Rev. D **45**, S1 (1992).

[13] A.L. Weinstein and R. Stroynowski, Annu. Rev. Nucl. Part. Phys. **43**, 457 (1993).

[14] W.J. Marciano, Phys. Rev. D **45**, R721 (1992).

[15] T.P. Cheng and L.-F. Li, Phys. Rev. D **44**, 1502 (1991).

[16] M.W. Goodman and E. Witten, Phys. Rev. D **31**, 3059 (1985).

[17] G. Feinberg and S. Weinberg, Phys. Rev. Lett. **3**, 111, 244(E) (1959); W.J. Marciano and A.I. Sanda, ibid. **78**, 1512 (1977).

[18] O. Shanker, Phys. Rev. D **20**, 1608 (1979).

[19] J. Bernabeu et al., Nucl. Phys. **B409**, 69 (1993).

[20] B. Dreher et al., Nucl. Phys. **A235**, 219 (1974); B. Frois and C.N. Papanicolas, Annu. Rev. Nucl. Sci. **37**, 133 (1987).

[21] K.W. Ford and J.G. Wills, Nucl. Phys. **35**, 295 (1962); R. Pla and J. Bernabeu, An. Fis. **67**, 455 (1971).

[22] LAMF Collaboration, R.D. Bolton et al., Phys. Rev. D **38**, 2077 (1988).

[23] U. Bellgardt et al., Nucl. Phys. **B299**, 1 (1988).

[24] TRIUMF Collaboration, S. Ahmad et al., Phys. Rev. D **38**, 2102 (1988).

[25] A. Halprin, S.T. Petcov, and S.P. Rosen, Phys. Lett. **125B**, 335 (1983); C.N. Leung and S.T. Petcov, ibid. **145B**, 416 (1984).

[26] A. Halprin et al., Phys. Rev. D **13**, 2567 (1976).

[27] A. Balysh et al., Phys. Lett. B **283**, 32 (1992).

[28] B. Pontecorvo, Sov. Phys. JETP **7**, 172 (1958); **26**, 984 (1968).

[29] Z. Maki et al., Prog. Theor. Phys. **28**, 870 (1962).

[30] C. Angelini et al., Phys. Lett. B **179**, 307 (1986).

[31] J. Pantaleone, Phys. Rev. D **49**, 2152 (1994).

[32] T. Inami and C.S. Lim, Prog. Theor. Phys. **65**, 297 (1981); **65**, 1772 (1981).

[33] J. Bernabeu, J.G. Korner, A. Pilaftsis, and K. Schilcher, Phys. Rev. Lett. **71**, 2695 (1993).

[34] S.T. Petcov, Sov. J. Nucl. Phys. **25**, 340 (1977); **25**, 698(E) (1977); Phys. Lett. **68B**, 364 (1977); T.P. Cheng and L.F. Li, Phys. Rev. D **16**, 1425 (1977); **16**, 1565 (1977).